

Infrared Spectra and Structures of the Coinage Metal Dihydroxide Molecules

Xuefeng Wang and Lester Andrews*

Department of Chemistry, University of Virginia, P.O. Box 400319, Charlottesville, Virginia 22904-4319

Received July 18, 2005

Laser-ablated Cu, Ag, and Au atoms react with H_2O_2 and with $\text{H}_2 + \text{O}_2$ molecules during condensation in excess argon to give four new IR absorptions in each system (O–H stretch, M–O–H bend, O–M–O stretch, and M–O–H deformation modes) that are due to the coinage metal $\text{M}(\text{OH})_2$ dihydroxide molecules. Isotopic substitution (D_2O_2 , $^{18}\text{O}_2$, $^{16}\text{O}^{18}\text{O}$, D_2 , and HD) and comparison with frequencies computed by DFT verify these assignments. The calculations converge to ${}^2\text{B}_g$ ground electronic state structures with C_{2h} symmetry, $111\text{--}117^\circ$ M–O–H bond angles, and substantial covalent character for these new metal dihydroxide molecules, particularly for $\text{Au}(\text{OH})_2$. This is probably due to the high electron affinity of gold owing to the effect of relativity.

Introduction

The coinage metals show decreasing chemical reactivity going down the family from copper to silver to gold. Gold is unreactive, but gold combines with strong chemical oxidizing agents such as chlorine or aqua regia.¹ Although binary gold compounds are limited to pairing with the most electronegative elements, stable gold hydrides have been prepared in spectroscopic quantities.^{2,3} Gold hydroxide molecules have not been observed experimentally, but relativistic calculations have recently been performed for AuOH .⁴ Gold aquoxide or hydroxide solid materials prepared by the electrochemical oxidation of gold anode surfaces in solutions are not well-defined, but $\text{Au}(\text{OH})_2^-$ is a possible hydrolysis product.⁵ A solid produced by cooling annealed gold films in H_2 and then O_2 was examined by early electron diffraction methods and determined to have the $\text{Au}(\text{OH})_2$ stoichiometry,⁶ but this work has not been substantiated. Monomeric gold(II) complexes are scarce, although the AuO

molecule has been observed in solid argon and in the gas phase, and AuH_2 has been prepared in solid hydrogen.^{7–10} The neutralization of aqueous gold chloride solutions (HAuCl_4) with Na_2CO_3 leads to an amorphous brown precipitate of gold(III) aquoxide, or $\text{Au}_2\text{O}_3 \cdot n\text{H}_2\text{O}$, which is sometimes called $\text{Au}(\text{OH})_3$.¹¹ In addition, the anion $\text{Au}(\text{OH})_4^-$ is thought to form in strongly basic solutions,^{1,5} and the crystal structures of two alkaline earth metal tetrahydroxoaurate(III) salts have been determined.¹² Finally, dimethyl gold(III) hydroxide is known as a tetrameric ring compound.¹³

Silver and copper, on the other hand, form monobasic hydroxides of moderate strength.¹ The CuOH and AgOH molecules have been characterized in the gas phase^{14–16} and by calculations at several levels of theory including relativistic effects.^{4,17} In addition, CuOH has been prepared in solid argon from the photochemical reaction of Cu and H_2O .¹⁸ Copper dihydroxide is obtained as a blue precipitate from

* Author to whom correspondence should be addressed. E-mail: isa@virginia.edu.

- (1) Cotton, F. A.; Wilkinson, G.; Murillo, C. A.; Bochmann, M. *Adv. Inorg. Chem.*, 6th ed.; Wiley: New York, 1999.
- (2) Huber, K. P.; Herzberg, G. *Molecular Spectra and Molecular Structure, Vol. IV, Constants of Diatomic Molecules*; Van Nostrand Reinhold: New York, 1979.
- (3) (a) Wang, X.; Andrews, L. *J. Am. Chem. Soc.* **2001**, *123*, 12899. (b) Andrews, L.; Wang, X. *J. Am. Chem. Soc.* **2003**, *125*, 11751.
- (4) Ikeda, S.; Nakajima, T.; Hirao, K. *Mol. Phys.* **2003**, *101*, 105.
- (5) *Gmelin Handbook on Inorganic and Organometallic Chemistry*, 8th ed., Gold, Suppl. B1; Springer: Berlin, 1992; pp 84–97 and references therein.
- (6) Baranova, R. V.; Khodyrev, Y. P.; Udalova, U. V. *Izv. Akad. Nauk SSSR, Ser. Fiz.* **1984**, *48*, 1654.

- (7) Citra, A.; Andrews, L. *THEOCHEM* **1999**, *489*, 95.
- (8) Okabayashi, T.; Koto, F.; Tsukamoto, K.; Yamazaki, E.; Tanimoto, M. *Chem. Phys. Lett.* **2005**, *403*, 223.
- (9) (a) Wang, X.; Andrews, L.; Manceron, L.; Marsden, C. *J. Phys. Chem. A* **2003**, *107*, 8492. (b) Andrews, L.; Wang, X.; Manceron, L.; Balasubramanian, K. *J. Phys. Chem. A* **2004**, *108*, 2936.
- (10) Pyykko, P. *Angew. Chem., Intl. Ed.* **2004**, *43*, 4412.
- (11) Schwarzmann, E.; Fellwock, E. *Z. Naturforsch.* **1971**, *26b*, 1369.
- (12) (a) Jones, P. G.; Sheldrick, G. M. *Acta Crystallogr., Sect. C* **1984**, *40*, 1776. (b) Jones, P. G.; Schelbach, R.; Schwarzmann, E. *Z. Naturforsch.* **1987**, *42b*, 522.
- (13) Glass, G. E.; Konner, J. H.; Miles, M. G.; Britton, D.; Tobias, R. S. *J. Am. Chem. Soc.* **1968**, *90*, 1131.
- (14) Trkula, M.; Harris, D. O. *J. Chem. Phys.* **1983**, *79*, 1138.
- (15) Jarman, C. N.; Fernando, W. T. M. L.; Bernath, P. F. *J. Mol. Spectrosc.* **1990**, *144*, 286; **1991**, *145*, 151.
- (16) Whitham, C. J.; Ozeki, H.; Saito, S. *J. Chem. Phys.* **2000**, *112*, 641.

alkali hydroxide and cupric ion solution, but warming dehydrates this compound to the oxide. However, $\text{Cu}(\text{OH})_2$ is soluble in concentrated strong base to give deep blue anions [such as $\text{Cu}(\text{OH})_4^{2-}$], but there is no evidence for pure solid $\text{Ag}(\text{OH})_2$.¹ In this paper, we report the preparation of copper, silver, and gold dihydroxide molecules through the reaction of excited metal atoms with hydrogen peroxide molecules and with mixtures of O_2 and H_2 . Similar reactions with H_2 have formed coinage metal hydrides, where monohydride species dominate the product yield,^{3,9} but in contrast, the metal dihydroxide is the major hydroxide molecule formed here. This is particularly noteworthy as the +2 oxidation state is less common for silver and gold. A preliminary communication on the $\text{Au}(\text{OH})_2$ molecule has been published.¹⁹

Experimental and Theoretical Methods

Experimentally, laser-ablated Cu, Ag, and Au atoms were reacted with H_2O_2 molecules in an argon stream during condensation onto a 10 K infrared transparent window, as described previously.^{3,20} Urea–hydrogen peroxide (Aldrich) at room temperature in the sidearm of a Chemglass Pyrex-Teflon valve provided H_2O_2 molecules to the flowing argon reaction medium (4 mmol in 60 min). A deuterium-enriched urea– D_2O_2 complex was prepared by adapting earlier procedures to exchange urea and H_2O_2 with D_2O .²¹ Argon matrix infrared spectra were recorded on a Nicolet 750 spectrometer after sample deposition, after annealing, and after irradiation by a mercury arc lamp (Philips, 175 W, globe removed). Experiments were also performed with H_2 and O_2 mixtures in order to introduce $^{18}\text{O}_2$ into the reaction products, as done for the alkaline earth metal dihydroxide molecules.²²

Theoretically, the structures and vibrational frequencies of the $\text{Cu}(\text{OH})_2$, $\text{Ag}(\text{OH})_2$, $\text{Au}(\text{OH})_2$, CuOH , AgOH , and AuOH molecules were calculated using methods employed for gold hydrides³ and mercury dihydroxide.^{23,24} The 6-311++G(3df,3pd) basis was used for H, O, and Cu. Relativistic effects were accounted for in the SDD pseudopotential and basis for silver and gold (19 valence

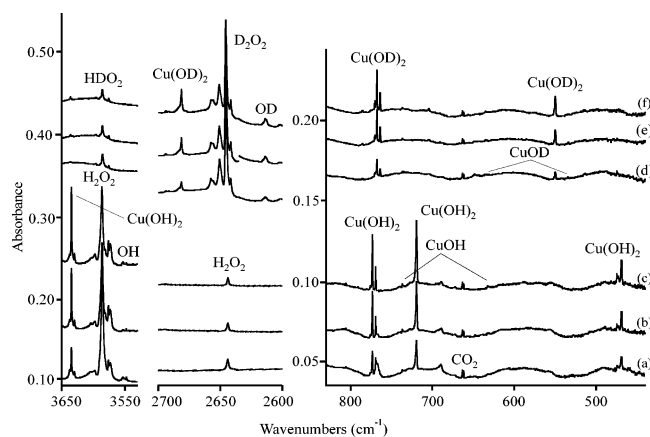


Figure 1. Infrared spectra for the copper and hydrogen peroxide reaction products in solid argon at 10 K. (a) $\text{Cu} + \text{H}_2\text{O}_2$ deposited for 60 min, (b) after 240–380 nm irradiation, and (c) after $\lambda > 220$ nm irradiation; (d) $\text{Cu} + \text{D}_2\text{O}_2$ deposited for 60 min, (e) after 240–380 nm irradiation, and (f) after $\lambda > 220$ nm irradiation.

electrons).²⁵ All geometrical parameters were fully optimized, and harmonic frequencies were calculated analytically at the optimized structures.

Results and Discussion

Reactions of coinage metal atoms with H_2O_2 and with $\text{H}_2 + \text{O}_2$ mixtures are investigated, and the major metal dihydroxide products are identified by matrix infrared spectroscopy through isotopic substitution and comparison to frequencies calculated by density functional theory.

Copper. Laser-ablated copper atoms were deposited with H_2O_2 in an argon stream during condensation at 10 K, and infrared spectra of this sample are illustrated in Figure 1. The strong 3586.2 and weaker 3576.3 and 3573.4 cm^{-1} bands are common to H_2O_2 experiments,^{21,23} but the sharp 3634.7 cm^{-1} band is unique to copper, as are the sharp bands at 773.5, 769.4, 719.4, and 468.8 cm^{-1} also labeled $\text{Cu}(\text{OH})_2$ in the lower wavenumber region. Annealing to 22 K sharpened but did not increase these new bands, whereas the H_2O_2 dimer absorptions increased about 20%, and the OH radical absorption at 3553.0 and 3548.0 cm^{-1} decreased as well.²⁶ Visible irradiation had no effect on the spectrum. However, ultraviolet (240–380 nm) irradiation exciting the copper $^2\text{S} \rightarrow ^2\text{P}$ transition²⁷ increased the above bands by 25%, and the more intense ultraviolet light in the full arc ($\lambda > 220$ nm) increased the bands another 20% (Figure 1b,c). The OCuO doublet at 823.1 and 818.7 cm^{-1} and weak CuOH bands at 727.5 and 632.5 cm^{-1} also increased on UV irradiation.^{18,28}

The analogous experiment with D_2O_2 gave 2651.3 and 2645.7 cm^{-1} bands common to D_2O_2 investigations²¹ and a sharp 2681.4 cm^{-1} band unique to copper along with sharp

- (17) (a) Illas, F.; Rubio, J.; Centellas, F.; Virgili, J. *J. Phys. Chem.* **1984**, *88*, 5225. (b) Bauschlicher, C. W. *Int. J. Quantum Chem. Symp.* **1986**, *20*, 563. (c) Mochizuki, Y.; Takada, T.; Murakami, A. *Chem. Phys. Lett.* **1991**, *185*, 535.
- (18) Kauffman, J. W.; Hauge, R. H.; Margrave, J. L. *J. Phys. Chem.* **1985**, *89*, 3541.
- (19) Wang, X.; Andrews, L. *Chem. Commun.* **2005**, 4001.
- (20) Andrews, L. *Chem. Soc. Rev.* **2004**, *33*, 123 and references therein.
- (21) (a) Pettersson, M.; Tuominen, S.; Rasanen, M. *J. Phys. Chem. A* **1997**, *101*, 1166. (b) Pehkonen, S.; Pettersson, M.; Lundell, J.; Khriachtchev, L.; Rasanen, M. *J. Phys. Chem. A* **1998**, *102*, 7643.
- (22) (a) Andrews, L.; Wang, X. *Inorg. Chem.* **2005**, *44*, 11. (b) Wang, X.; Andrews, L. *J. Phys. Chem. A* **2005**, *109*, 2782.
- (23) (a) Wang, X.; Andrews, L. *Inorg. Chem.* **2005**, *44*, 108. (b) Wang, X.; Andrews, L. *J. Phys. Chem. A* **2005**, *109*, 3849.
- (24) Frisch, M. J.; Trucks, G. W.; Schlegel, H. B.; Scuseria, G. E.; Robb, M. A.; Cheeseman, J. R.; Zakrzewski, V. G.; Montgomery, J. A., Jr.; Stratmann, R. E.; Burant, J. C.; Dapprich, S.; Millam, J. M.; Daniels, A. D.; Kudin, K. N.; Strain, M. C.; Farkas, O.; Tomasi, J.; Barone, V.; Cossi, M.; Cammi, R.; Mennucci, B.; Pomelli, C.; Adamo, C.; Clifford, S.; Ochterski, J.; Petersson, G. A.; Ayala, P. Y.; Cui, Q.; Morokuma, K.; Malick, D. K.; Rabuck, A. D.; Raghavachari, K.; Foresman, J. B.; Cioslowski, J.; Ortiz, J. V.; Stefanov, B. B.; Liu, G.; Liashenko, A.; Piskorz, P.; Komaromi, I.; Gomperts, R.; Martin, R. L.; Fox, D. J.; Keith, T.; Al-Laham, M. A.; Peng, C. Y.; Nanayakkara, A.; Gonzalez, C.; Challacombe, M.; Gill, P. M. W.; Johnson, B. G.; Chen, W.; Wong, M. W.; Andres, J. L.; Head-Gordon, M.; Replogle, E. S.; Pople, J. A. *Gaussian 98*, revision A.6; Gaussian, Inc.: Pittsburgh, PA, 1998.

- (25) Schwerdtfeger, P.; Schwarz, W. H. E.; Bowmaker, G. A.; Boyd, P. D. W. *J. Chem. Phys.* **1989**, *91*, 1762.
- (26) Cheng, B.-M.; Lee, Y.-P.; Ogilvie, J. F. *Chem. Phys. Lett.* **1988**, *109*, 151.
- (27) (a) Vala, M.; Zeringue, K.; Shakh's Emampour, J.; Rivoal, J.-C.; Pyzalski, R. *J. Chem. Phys.* **1984**, *80*, 2401. (b) Ozin, G. A.; Gracie, C. *J. Phys. Chem.* **1984**, *88*, 643.
- (28) Chertihin, G. V.; Andrews, L.; Bauschlicher, C. W., Jr. *J. Phys. Chem. A* **1997**, *101*, 4026.

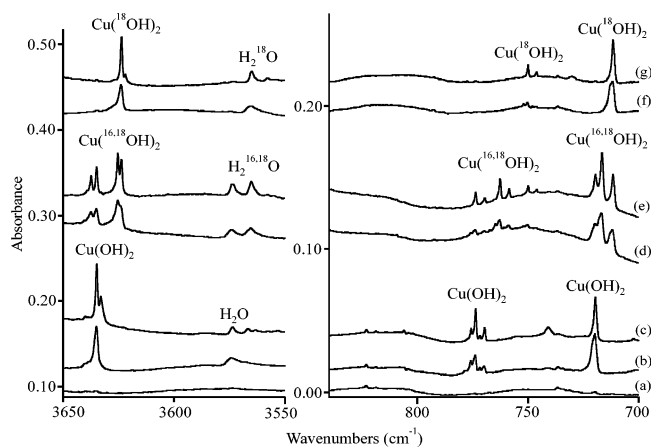


Figure 2. Infrared spectra for the copper, oxygen, and hydrogen reaction products in solid argon at 10 K. (a) Cu + 0.4% O₂ + 6% H₂ deposited for 60 min, (b) after $\lambda > 220$ nm irradiation, and (c) after annealing to 20 K; (d) Cu + 0.1% ¹⁶O₂ + 0.2% ¹⁶O¹⁸O + 0.1% ¹⁸O₂ + 6% H₂ deposited and irradiated with $\lambda > 220$ nm irradiation and (e) after annealing to 22 K; (f) Cu + 0.2% ¹⁸O₂ + 6% H₂ deposited and irradiated with $\lambda > 220$ nm and (g) after annealing to 24 K.

associated bands at 767.9, 763.9, and 549.8 cm⁻¹. These bands exhibited the same annealing and photolysis behavior as their H₂O₂ counterparts. A sharp, weak 3636.2 cm⁻¹ band was observed from HDO₂ in the D₂O₂ sample. Weak CuOD bands were also observed at 635.1 and 533.5 cm⁻¹.¹⁸

The sharp doublet at 773.5 and 769.4 cm⁻¹ exhibits the 2.3–1.0 relative intensity for ⁶³Cu and ⁶⁵Cu in natural abundance and demonstrates the participation of a single Cu atom in the new product molecule. Furthermore, the magnitude of the ⁶³Cu and ⁶⁵Cu isotopic shift indicates that copper is vibrating between two oxygen masses (63/65 frequency ratio 1.0053) and not against a single oxygen mass as in the diatomic CuO molecule (63/65 ratio 1.0031).²⁸

Experiments were performed with Cu and H₂ + O₂ mixtures in order to introduce ¹⁸O into the new product molecule. Infrared spectra are compared in Figure 2; the deposited samples contain common HO₂ and Ar_nH⁺ bands,^{29–32} and weak product absorptions, but full arc irradiation increases the latter bands, and annealing sharpens new absorptions at 3634.9, 773.67, 769.59, and 719.6 cm⁻¹, which are 0.2 cm⁻¹ higher than the Cu and H₂O₂ reaction products. The reaction with ¹⁸O₂ gives substantial shifts with new absorptions at 3623.7, 750.0, 746.1, and 711.6 cm⁻¹, as listed in Table 1. The H₂ and ¹⁶O₂ + ¹⁶O¹⁸O + ¹⁸O₂ reagent produced diagnostic isotopic multiplet absorptions. The triplet of copper isotopic doublets with new ¹⁶O¹⁸O components at 762.6 and 758.5 cm⁻¹ verifies the participation of *two equivalent* oxygen atoms, as does the triplet at 719.6, 716.6, and 711.6 cm⁻¹. The new absorptions at 3637.3 and 3625.4 cm⁻¹, in addition to the pure isotopic bands at 3634.9 and 3623.7 cm⁻¹, arise because both (¹⁶O–H) and (¹⁸O–H) stretching modes are active in the new mixed isotopic product, which must, therefore, contain two OH subunits.

The participation of two OH subunits is confirmed by the reaction of Cu and HD + O₂, and spectra for H₂, HD, and

D₂ + O₂ reactions with Cu are compared in Figure 3. The new product absorptions with D₂ + O₂ at 2681.5, 768.04, 764.02, and 549.8 cm⁻¹ are within 0.1 cm⁻¹ of the absorptions formed with D₂O₂ as the reagent. The HD + O₂ mixture gave the following diagnostic information: (a) an intermediate copper isotope doublet at 770.42 and 766.33 cm⁻¹, (2) two bending modes at 704.4 and 526.0 cm⁻¹, (3) a new O–H stretching mode at 3636.3 cm⁻¹, which is 1.5 cm⁻¹ higher than the frequency with H₂, and (4) a new O–D stretching mode at 2684.1 cm⁻¹, which is 2.6 cm⁻¹ higher than the frequency with D₂.

Hence, we have identified the new Cu(OH)₂ molecule from four vibrational modes (O–H stretch, O–Cu–O stretch, Cu–O–H bend, and Cu–O–H out-of-plane deformation). Mixed isotopic precursors have verified the participation of two O–H(O–D) oscillators, two equivalent O atoms, and a single Cu atom in this new dihydroxide molecule.

The assignments to Cu(OH)₂ are confirmed by the match of frequencies and isotopic shifts computed by density functional theory. Table 1 compares the observed and calculated frequencies. First, the ground-state molecule is converged to be a planar ²B_g state with C_{2h} symmetry, as shown in Figure 4, and only *ungerade* modes are allowed in the IR spectrum. Second, the four strongest infrared-active fundamentals calculated are observed in the spectrum: the calculated O–H stretching and Cu–O–H bending and deformation modes are 5.1, 0.5, and 10.3% higher than observed, but the calculated O–Cu–O stretching mode is 0.8% lower than observed. Third, the calculated and observed isotopic shifts agree very well: the calculated and observed ⁶³Cu–⁶⁵Cu shift for the b_u O–Cu–O mode are both 4.1 cm⁻¹, but the calculated ¹⁶O–¹⁸O shift (26.7 cm⁻¹) slightly exceeds the observed value (23.7 cm⁻¹), whereas the calculated H–D shift (3.5 cm⁻¹) is just below the observed value (5.7 cm⁻¹). This almost pure antisymmetric O–Cu–O stretching mode is described accurately but not perfectly by the B3LYP calculation. The ¹⁶O–Cu–¹⁸O counterpart is predicted to be 14.5/26.7 = 0.543 = 54.3% of the way up from ¹⁸O–Cu–¹⁸O to ¹⁶O–Cu–¹⁶O and observed to be 12.6/23.7 = 0.532 = 53.2% of the way up. The calculated b_u ¹⁶O–H/¹⁸O–H frequency ratio (1.003 27) slightly exceeds the observed ratio (1.003 09). In the Cu(¹⁶OH)(¹⁸OH) molecule of lower symmetry, both O–H stretching modes are observed, and they couple slightly sharing the intensity for their double statistical population in the ¹⁶O₂ + ¹⁶O¹⁸O + ¹⁸O₂ isotopic sample. The weaker ¹⁶O–H (more symmetric) mode is predicted to be 1.6 cm⁻¹ higher than the b_u Cu(¹⁶OH)₂ value, and it is observed to be 2.4 cm⁻¹ higher, whereas the stronger ¹⁸O–H (more antisymmetric) mode is predicted to be 2.3 cm⁻¹ higher than the b_u mode for Cu(¹⁸OH)₂ and is observed to be 1.7 cm⁻¹ higher. Likewise, in the Cu(OH)(OD) molecule, both O–H and O–D stretching modes are observed as predicted. In addition, both Cu–O–H and Cu–O–D bending modes are allowed in this molecule of lower symmetry, and both are observed.

(29) Milligan, D. E.; Jacox, M. E. *J. Chem. Phys.* **1963**, *38*, 2627.

(30) Smith, D. W.; Andrews, L. *J. Chem. Phys.* **1974**, *60*, 81.

(31) Milligan, D. E.; Jacox, M. E. *J. Mol. Spectrosc.* **1973**, *46*, 460.

(32) Wight, C. A.; Ault, B. S.; Andrews, L. *J. Chem. Phys.* **1976**, *65*, 1244.

Table 1. Observed and Calculated Frequencies (cm^{-1}) for $\text{Cu}(\text{OH})_2$ in the C_{2h} Structure

mode	$\text{Cu}(\text{OH})_2$		$\text{Cu}(\text{OH})(\text{OD})$		$\text{Cu}(\text{OD})_2$		$\text{Cu}({}^{18}\text{OH})_2$	
	obsd ^a	calcd ^b	obsd	calcd	obsd	calcd	obsd	calcd
O–H stretch		3836.0 (a_g , 0) ^{c,d}	3636.3	3834.0 (127)		2792.9 (0)		3823.4 (0)
O–H stretch	3634.9	3832.0 (b_u , 256)	2684.1	2791.4 (76)	2681.5	2789.8 (152)	3623.7	3819.5 (250)
O–Cu–O stretch	773.7	767.5 (b_u , 98)	770.4	765.7 (110)	768.0	764.0 (118)	750.0	740.8 (44)
Cu–O–H bend	719.6	722.9 (b_u , 197)	704.4	710.1 (105)		613.2 (0)	711.6	717.7 (240)
Cu–O–H bend		695.3 (a_g , 0)		612.8 (5)	549.8	541.5 (92)		691.7 (0)
O–Cu–O stretch		609.6 (a_g , 0)	526.0	517.8 (32)		498.4 (0)		576.3 (0)
Cu–O–H deform	468.8	517.5 (a_u , 176)		460.2 (141)		394.5 (107)		513.4 (173)
O–Cu–O bend, in		187.2 (b_u , 11)		181.6 (11)		176.2 (11)		181.4 (11)
O–Cu–O bend, out		109.8 (a_u , 1)		106.5 (1)		103.0 (1)		106.5 (1)

^a Observed in solid argon. ^b Calculated at B3LYP/6-311++G(3df,3pd) level of theory. ^c Mode symmetry in C_{2h} , infrared intensity, km/mol . ^d Strong absorptions calculated for $\text{Cu}({}^{16}\text{OH})({}^{18}\text{OH})$ are 3834.3 (90), 3821.1 (163), 755.3 (79), 720.9 (208), and 515.4 cm^{-1} (175 km/mol).

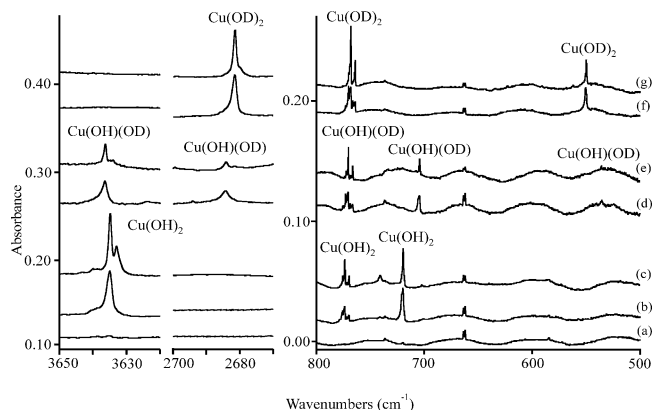


Figure 3. Infrared spectra for the copper, oxygen, and hydrogen peroxide reaction products in solid argon at 10 K. (a) $\text{Cu} + 0.4\% \text{O}_2 + 6\% \text{H}_2$ deposited for 60 min. (b) after $\lambda > 220 \text{ nm}$ irradiation, and (c) after annealing to 24 K; (d) $\text{Cu} + 0.4\% \text{O}_2 + 6\% \text{HD}$ deposited and irradiated with $\lambda > 220 \text{ nm}$ irradiation and (e) after annealing to 30 K; (f) $\text{Cu} + 0.4\% \text{O}_2 + 6\% \text{D}_2$ deposited and irradiated with $\lambda > 220 \text{ nm}$ irradiation and (g) after annealing to 24 K.

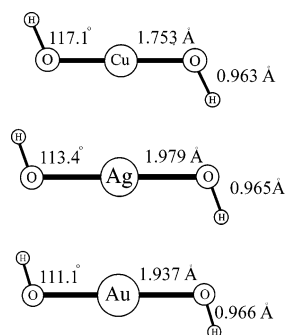


Figure 4. C_{2h} structures computed for the $\text{Cu}(\text{OH})_2$, $\text{Ag}(\text{OH})_2$, and $\text{Au}(\text{OH})_2$ molecules at the B3LYP/6-311++G(3df,3dp) level of theory using the SDD pseudopotential for Ag and Au.

The CuOH and CuOD monohydroxide molecules are observed, here, as weak bands for bending and $\text{Cu}-\text{O}$ stretching modes, in agreement with previous matrix isolation work.¹⁸ The stronger bending mode measured in the gas phase for CuOH and CuOD is 15 and 3 cm^{-1} higher,¹⁴ and the argon matrix values sustain a reasonable matrix shift.

Silver. Laser-ablated silver atoms were reacted with H_2O_2 during condensation in excess argon, and infrared spectra are illustrated in Figure 5. The metal-dependent bands labeled $\text{Ag}(\text{OH})_2$ now appear at 3582.3 and 702.7 cm^{-1} and very weakly at 614.6 and 454.0 cm^{-1} . As with copper, the silver product bands increase on UV irradiation. In addition, a new,

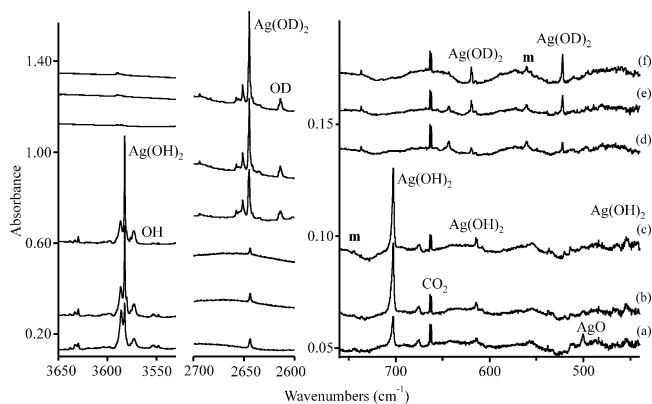


Figure 5. Infrared spectra for the silver and hydrogen peroxide reaction products in solid argon at 10 K. (a) $\text{Ag} + \text{H}_2\text{O}_2$ deposited for 60 min, (b) after 240–380 nm irradiation, and (c) after $\lambda > 220 \text{ nm}$ irradiation; (d) $\text{Ag} + \text{D}_2\text{O}_2$ deposited for 60 min, (e) after 240–380 nm irradiation, and (f) after $\lambda > 220 \text{ nm}$ irradiation.

very weak band was observed at 744.3 cm^{-1} (labeled **m** for monohydroxide AgOH). The Ag reaction with D_2O_2 shifted these absorptions to 2644.7, 522.4, and 619.5 cm^{-1} and to 538.5 cm^{-1} , and a weak HDO_2 reaction product was observed at 3589.7 cm^{-1} . The Ag and $\text{H}_2 + \text{O}_2$ reaction was performed for ${}^{18}\text{O}_2$ substitution, and the stronger product bands shifted to 3571.3, 699.2, and 589.9 cm^{-1} , as listed in Table 2. Reaction with H_2 and ${}^{16}\text{O}_2 + {}^{16}\text{O}{}^{18}\text{O} + {}^{18}\text{O}_2$ gave a quartet at 3594.4, 3582.3, 3575.1, and 3571.3 cm^{-1} and a triplet at 702.7, 700.9, and 699.2 cm^{-1} . Reaction with $\text{D}_2 + \text{O}_2$ gave the same stronger bands as D_2O_2 , but the $\text{HD} + \text{O}_2$ reaction produced new absorptions at 3589.3, 2651.0, 689.8, and 523.4 cm^{-1} . The mixed isotopic experiments identify a new Ag -containing molecule with two $\text{OH}(\text{OD})$ groups and two equivalent oxygen atoms, and $\text{Ag}(\text{OH})_2$ is, thus, identified.

Like $\text{Cu}(\text{OH})_2$, the ground state of $\text{Ag}(\text{OH})_2$ is calculated to be 2B_g in C_{2h} symmetry, and the agreement between observed and calculated frequencies displayed in Table 2 attests to this assignment. The calculation using the SDD pseudopotential for silver predicts the $\text{O}-\text{H}$ stretching 6.1% too high, the $\text{Ag}-\text{O}-\text{H}$ bending mode 2.6% too high, the $\text{O}-\text{Ag}-\text{O}$ stretching mode 6.6% lower and weaker than observed, and the $\text{Ag}-\text{O}-\text{H}$ deformation mode 9.1% too high, which is not as good as the agreement found for $\text{Cu}(\text{OH})_2$ using the all-electron basis for copper. The calculation does correctly predict the blue deuterium shift for the $\text{O}-\text{Ag}-\text{O}$ stretching mode. The b_u $\text{Ag}-\text{O}-\text{H}$ bending and

Table 2. Observed and Calculated Frequencies (cm^{-1}) for $\text{Ag}(\text{OH})_2$ in the C_{2h} Structure

mode	$\text{Ag}(\text{OH})_2$		$\text{Ag}(\text{OH})(\text{OD})$		$\text{Ag}(\text{OD})_2$		$\text{Ag}({}^{18}\text{OH})_2$	
	obsd ^a	calcd ^b	obsd	calcd	obsd	calcd	obsd	calcd
O–H stretch		3808.7 ($a_g, 0$) ^{c,d}	3589.8	3805.2 (225)		2772.8 (0)		3796.1
O–H stretch	3582.3	3801.7 ($b_u, 452$)	2651.0	2770.4 (122)	2644.7	2768.0 (243)	3571.3	3789.1
Ag–O–H bend	702.7	731.1 ($b_u, 245$)	689.8	719.2 (137)	619.5	596.7 (81)	699.2	726.4
Ag–O–H bend		705.0 ($a_g, 0$)	616.2	585.5 (25)		530.2 (0)		701.9
O–Ag–O stretch	614.6	576.4 ($b_u, 2$)	523.4	524.9 (29)	522.4	518.2 (58)	589.9	553.0
Ag–O–H deform	454.0	495.5 ($a_u, 160$)		448.5 (3)		374.3 (94)		491.9
O–Ag–O stretch		459.5 ($a_g, 0$)		439.2 (127)		438.9 (0)		434.3
O–Ag–O bend, in		142.6 ($b_u, 6$)		139.0 (6)		135.5 (6)		137.2
O–Ag–O bend, out		68.1 ($a_u, 1$)		67.0 (0)		64.2 (0)		65.6

^a Observed in solid argon. ^b Calculated at B3LYP/6-311++G(3df,3pd)/SDD level of theory. ^c Mode symmetry in C_{2h} , infrared intensity, km/mol . ^d Strong absorptions calculated for $\text{Ag}({}^{16}\text{OH})({}^{18}\text{OH})$ are 3806.1 (117), 3791.7 (334), 728.9 (241), 565.9 (3), and 493.6 cm^{-1} (158 km/mol).

O–Ag–O stretching modes are near enough to mix, and upon deuteration, the Ag–O–D bending mode shifts below the O–Ag–O stretch and forces it to higher wavenumbers, although the observed interaction is not as much as predicted. As for copper, the quartet of O–H stretching modes is predicted for the silver and ${}^{16}\text{O}_2 + {}^{16}\text{O}^{18}\text{O} + {}^{18}\text{O}_2$ reaction product, although the observed splittings are slightly more than calculated. Likewise, the O–H and O–D stretching modes for $\text{Ag}(\text{OH})(\text{OD})$ are predicted above the pure isotopic bands as observed, and the Ag–O–H and Ag–O–D bending modes are both observed.

The weak, new bands at 744.3 and 538.5 cm^{-1} , just above the strong bending modes for $\text{Ag}(\text{OH})_2$ and $\text{Ag}(\text{OD})_2$, have the ratio 1.3822, which is appropriate for the bending modes of AgOH and AgOD . The AgOH bands have been calculated at 766 cm^{-1} at the DK3-CCSD(T) level⁴ and at 787 cm^{-1} as the strongest IR absorption at the B3LYP level,³³ which supports the assignment of the above weak bands to AgOH and AgOD . Our calculation for CuOH also gives parameters³³ in good agreement with the previous higher-level calculation.⁴

Gold. Infrared spectra of the $\text{Au} + \text{H}_2\text{O}_2$ reaction products are illustrated in Figure 6. The major, new absorptions at 3565.9, 884.9, 676.6, and 532.5 cm^{-1} [labeled $\text{Au}(\text{OH})_2$] increased substantially upon UV irradiation, but weaker bands at 3571.3 and 840.8 cm^{-1} increased only slightly. Annealing the sample to 20 K decreases the 3571.3 and 840.8 cm^{-1} absorptions with no effect on the former bands. Near-ultraviolet (240–380 nm) and full-arc ($\lambda > 220$ nm) irradiation markedly increased the former absorptions (Figure 6b,c) and slightly increased a weak, new 931.0 cm^{-1} band (labeled **m** for monohydroxide AuOH), a weak OAuO band^{7,34} at 817.9 cm^{-1} , the 3571.3 and 840.8 cm^{-1} pair, and a weak AuH absorption³ at 2226.6 cm^{-1} , and subsequent annealing to 30 K decreased these bands by about 30%. The gold atom reaction was also done with D_2O_2 , and Figure 6 also presents representative spectra. The major, new absorptions [labeled $\text{Au}(\text{OD})_2$] shifted as listed in Table 3.

Complementary experiments were performed with $\text{H}_2 + \text{O}_2$ as the reagent, and infrared spectra are shown in Figure

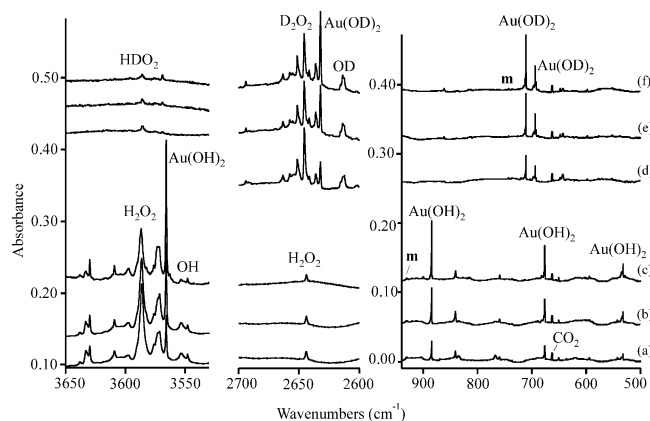


Figure 6. Infrared spectra for the gold and hydrogen peroxide reaction products in solid argon at 10 K. (a) $\text{Au} + \text{H}_2\text{O}_2$ deposited for 60 min, (b) after 240–380 nm irradiation, and (c) after $\lambda > 220$ nm irradiation; (d) $\text{Au} + \text{D}_2\text{O}_2$ deposited for 60 min, (e) after 240–380 nm irradiation, and (f) after $\lambda > 220$ nm irradiation.

7. Deposition with laser-ablated Au atoms gave weak product bands including OAuO ,^{7,34} but UV irradiation increased these absorptions at essentially the same wavenumbers observed with H_2O_2 . The major product absorptions were about 4 times stronger with H_2O_2 . Spectra with the $\text{H}_2 + {}^{16}\text{O}_2 + {}^{16}\text{O}^{18}\text{O} + {}^{18}\text{O}_2$ reagent mixture produced multiplet absorptions near 3560, 880, and 660 cm^{-1} . Investigations were also done with $\text{D}_2 + \text{O}_2$ and $\text{D}_2 + {}^{18}\text{O}_2$ mixtures, and shifted product absorptions were observed in each case. Experiments with HD and O_2 gave the unique mixed H/D product with new absorptions (Table 3). Figure S1 (Supporting Information) compares spectra of deuterated reaction products.

The sharp major reaction product absorptions at 3565.9, 884.9, 676.6, and 532.5 cm^{-1} are grouped by common behavior upon photolysis and annealing and formation from both H_2O_2 and $\text{H}_2 + \text{O}_2$ reagents at several sample concentrations. From the higher IR frequencies, O–H stretching and Au–O–H bending modes are identified.¹⁹ Next, the 676.6 cm^{-1} absorption shifts to 645.7 cm^{-1} with ${}^{18}\text{O}_2$ (16/18 ratio 1.0478), and the band becomes an asymmetric triplet at 676.6, 666.2, and 645.7 cm^{-1} with statistical ${}^{16,18}\text{O}_2$, which is precisely what is observed for the antisymmetric stretching mode of the linear O–Au–O molecule (16/18 ratio 1.0506).^{7,34} Hence, the new molecule contains an O–Au–O subunit with equivalent oxygen atoms. Accordingly, the isotopic vibrational spectra definitively identify the new molecule $\text{Au}(\text{OH})_2$.¹⁹

(33) (a) B3LYP calculation for AgOH . Structure: Ag–O, 2.042 Å; O–H, 0.963 Å, angle 107.4°. Frequencies: 3826 cm^{-1} (36 km/mol), 787 cm^{-1} (63 km/mol), 483 cm^{-1} (31 km/mol). (b) B3LYP calculation for CuOH using SDD. Structure: Cu–O, 1.780 Å; O–H, 0.963 Å, angle 109.0°. Frequencies: 3820 cm^{-1} (42 km/mol), 810 cm^{-1} (78 km/mol), 609 cm^{-1} (37 km/mol).

(34) Wang, X.; Andrews, L. *J. Phys. Chem. A* **2001**, *105*, 5812.

Table 3. Observed and Calculated Frequencies (cm^{-1}) for $\text{Au}(\text{OH})_2$ in the C_{2h} Structure

mode	$\text{Au}(\text{OH})_2$		$\text{Au}(\text{OH})(\text{OD})$		$\text{Au}(\text{OD})_2$		$\text{Au}(^{18}\text{OH})_2$		$\text{Au}(^{18}\text{OD})_2$	
	obsd ^a	calcd ^b	obsd	calcd	obsd	calcd	obsd	calcd	obsd	calcd
O–H stretch		3783.0 (a_g , 0) ^{c,d}	3569.1	3779.7 (167)		2753.9 (0)		3770.5		2736.7
O–H stretch	3565.9	3776.4 (b_u , 335)	2635.5	2751.4 (94)	2632.3	2748.9 (187)	3555.1	3764.0	2616.5	2731.8
Au–O–H bend	884.9	906.5 (b_u , 218)	862.1	888.3 (127)	711.3	708.6 (170)	879.0	900.3	686.5	668.8
Au–O–H bend		865.9 (a_g , 0)	692.6	682.8 (82)		651.1 (0)		862.6		637.6
O–Au–O stretch	676.6	641.2 (b_u , 39)		619.7 (5)	648.1	601.7 (1)	645.7	611.7	612.9	584.8
O–Au–O stretch		590.4 (a_g , 0)		573.9 (1)		563.8 (0)		557.7		541.0
Au–O–H deform	532.5	555.5 (a_u , 158)	474.4	491.5 (123)		417.6 (87)	530.7	551.7		412.2
O–Au–O bend, in		194.7 (b_u , 6)		189.3 (6)		184.0 (6)		186.3		177.1
O–Au–O bend, out		121.0 (a_u , 0)		119.0 (0)		114.4 (0)		115.9		110.2

^a Observed in solid argon. ^b Calculated at B3LYP/6-311++G(3df,3pd)/SDD level of theory. ^c Mode symmetry in C_{2h} , infrared intensity, km/mol . ^d Strong absorptions calculated for $\text{Au}(^{16}\text{OH})(^{18}\text{OH})$ are 3780.5 (89), 3766.5 (244), 903.5 (213), 630.7 (36), and 553.6 cm^{-1} (158 km/mol).

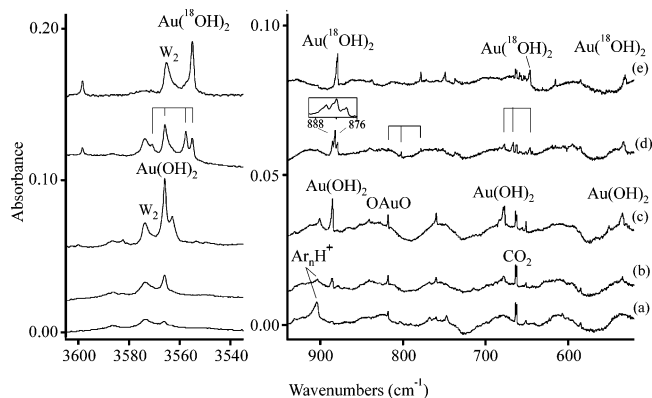


Figure 7. Infrared spectra for the gold, oxygen, and hydrogen reaction products in solid argon at 10 K. (a) Au + 0.4% O_2 + 6% H_2 deposited for 60 min, (b) after 240–380 nm irradiation, and (c) after $\lambda > 220$ nm irradiation; (d) Au + 0.1% $^{16}\text{O}_2$ + 0.2% $^{16}\text{O}^{18}\text{O}$ + 0.1% $^{18}\text{O}_2$ + 6% H_2 deposited and irradiated with $\lambda > 220$ nm; (e) Au + 0.4% $^{18}\text{O}_2$ + 6% H_2 deposited and irradiated with $\lambda > 220$ nm. W_2 denotes water dimer absorptions.

The vibrational assignments to $\text{Au}(\text{OH})_2$ are substantiated by excellent agreement between calculated and observed isotopic frequencies, and this agreement likewise confirms that the computed C_{2h} structure is the ground-state configuration of $\text{Au}(\text{OH})_2$. Calculations for the $\text{Au}(\text{OH})_2$ molecule converged to the C_{2h} structure illustrated in Figure 4 and provided the frequencies listed in Table 3. Notice that the three modes involving O–H stretching and bending are predicted to be 5.9, 2.4, and 4.3% too high by the B3LYP calculation, which is the expected relationship.³⁵ However, the O–Au–O mode prediction is low (5.2%), just as was found for $\text{Hg}(\text{OH})_2$ (4.8% low), $\text{Cu}(\text{OH})_2$, and $\text{Ag}(\text{OH})_2$. The $\text{Au}(\text{OH})_2$ molecule was also calculated with the BPW91 density functional, and the structure was essentially the same (1.947 Å, 0.975 Å, and 108.8°), but the frequencies were slightly lower, as expected.³⁵

The B3LYP calculation predicts the unobserved a_g O–H(D) stretching modes for $\text{Au}(\text{OH})_2$ and $\text{Au}(\text{OD})_2$ to be higher than the strong observed b_u modes. This means that the uncoupled O–H and O–D stretching modes in $\text{Au}(\text{OH})$ -(OD) will be higher than the observed b_u bands by half of the a_g – b_u mode separation, and that is precisely what is observed and calculated (Table 3). Furthermore, the calculation indicates coupling between the ^{16}O –H and ^{18}O –H

stretching modes in $\text{Au}(^{16}\text{OH})(^{18}\text{OH})$ and the asymmetric triplet mixed isotopic O–Au–O stretching mode, in agreement with the observed band separations. In summary, the B3LYP calculation accurately predicts subtle details in the spectra of mixed isotopic molecules, which provides further substantiation for the observation and characterization of $\text{Au}(\text{OH})_2$.

The weaker bands at 3571.3 and 840.8 cm^{-1} (Figure 6) shift to 3561.0 and 837.1 cm^{-1} with $^{18}\text{O}_2$ and to 2636.3 and 693.9 cm^{-1} with D_2O_2 (H/D ratios 1.3547 and 1.2117) and are also due to O–H stretching and Au–O–H bending modes. These bands decrease upon first annealing and increase only 30% upon UV irradiation. Our B3LYP calculation predicts almost the same energy C_{2v} $\text{Au}(\text{OH})_2$ structure with a strong O–H stretching mode 12 cm^{-1} higher and a Au–O–H bending mode 36 cm^{-1} lower than those for the C_{2h} structure. The weaker 3571.3 and 840.8 cm^{-1} bands are in good agreement with this relationship, and these bands are assigned to the minor population of $\text{Au}(\text{OH})_2$ trapped in the C_{2v} structure.

Relativistic calculations predict the AuOH triatomic molecule to have the 3727, 955, and 569 cm^{-1} frequencies,⁴ and our B3LYP/SDD results of 3793 cm^{-1} (65 km/mol infrared intensity), 957 cm^{-1} (60 km/mol), and 513 cm^{-1} (26 km/mol) and the structure are in excellent agreement.³⁶ The strong bending mode of AuOH is, thus, predicted to be 51 cm^{-1} higher than this bending mode for $\text{Au}(\text{OH})_2$ in the C_{2h} structure, and the new 931.0 cm^{-1} band is 46 cm^{-1} higher. The weak 931.0 cm^{-1} band and the deuterium counterpart at 743.2 cm^{-1} (H/D ratio 1.2527) are produced upon co-deposition with H_2O_2 and D_2O_2 , and they increase slightly upon UV irradiation. The 931.0 cm^{-1} band is favored relative to $\text{Au}(\text{OH})_2$ in experiments with less total H_2O_2 . These bands are appropriate for assignment to AuOH and AuOD, which provides the first experimental evidence for the gold monohydroxide molecule.

The $\text{Au}(\text{OH})_2^-$ molecular anion is isoelectronic with $\text{Hg}(\text{OH})_2$, and our calculated dihedral C_2 structures are almost the same.^{23,37} In contrast, $\text{Au}(\text{OH})_4^-$ is computed to have a planar C_{4h} structure with slightly shorter Au–O bond lengths

(36) B3LYP calculation for AuOH. Structure: Au–O, 1.990 Å; O–H, 0.966 Å, angle 104.6°. Frequencies: 3793 cm^{-1} (65 km/mol), 957 cm^{-1} (60 km/mol), 513 cm^{-1} (26 km/mol).

(37) At the B3LYP/6-311++G(3df, 3pd)/SDD level of theory, $\text{Au}(\text{OH})_2^-$ has the C_2 structure with Au–O, 2.045 Å; O–H, 0.961 Å; Au–O–H angle, 105.0°; O–Au–O angle, 176.9°; and dihedral angle, 90°.

(35) Scott, A. P.; Radom, L. *J. Phys. Chem.* **1996**, *100*, 16502.

(2.022 Å), and these gold hydroxide anions are discussed in the Supporting Information.

Family Trends. Several comparisons within the coinage metal family are of interest. All form the $M(\text{OH})_2$ dihydroxide molecules with C_{2h} symmetry structures as major products, and all give a small yield of the monohydroxide. Our observation of the same CuOH absorptions from Cu photochemical reactions with H_2O_2 and D_2O_2 , as found with H_2O and D_2O in solid argon,¹⁸ support these assignments and the slightly higher bending mode (743, 537 cm^{-1}) measurements in the gas phase¹⁴ for CuOH and CuOD . This agreement lends credence to our similar identifications of AgOH and AgOD , and of AuOH and AuOD , from reactions with H_2O_2 and D_2O_2 . Gold alone forms a minor C_{2v} isomer $\text{Au}(\text{OH})_2$ molecule. Absorptions are observed for OCuO and OAuO , as found before, but not for OAgO .^{7,28,34} Weak MH absorptions are observed for all metals in the experiments with $\text{H}_2 + \text{O}_2$; however, we have no evidence for CuOO , but the AgO_2 complex was strong, and AuOO was detected as reported previously.⁷ This indicates that Cu is the most reactive and Ag is the least reactive under the conditions of these experiments.

Natural charges, bond orbital analysis,^{38,39} and structures for $\text{Cu}(\text{OH})_2$, $\text{Ag}(\text{OH})_2$, and $\text{Au}(\text{OH})_2$ are presented in Table S1 (Supporting Information) and Figure 4. Although the O–H stretching frequency is lowest for $\text{Au}(\text{OH})_2$, the computed charge on gold and the Au–O–H angle are smallest, which suggests increasing covalent character from $\text{Cu}(\text{OH})_2$ to $\text{Ag}(\text{OH})_2$ to $\text{Au}(\text{OH})_2$. Note that the s electron population is substantially higher on gold, and the O–H bond length is longest for gold as well. A straightforward rationale for the increase in covalent character in the coinage metal dihydroxide series from Cu to Ag to Au is the increase in electron affinities of the metal atoms (28, 30, and 53 kcal/mol, respectively).⁴⁰ Thus, the high degree of covalent character in the $\text{Au}(\text{OH})_2$ molecule is probably due, in large part, to the high electron affinity of gold, which comes from relativity.¹⁰ One must remember that the OH (3568 cm^{-1})² and OH^- (3556 cm^{-1})⁴¹ fundamentals are so close that the O–H stretching frequency itself is not a measure of ionic character. A similar relationship has been found for the $\text{Zn}(\text{OH})_2$, $\text{Cd}(\text{OH})_2$, and $\text{Hg}(\text{OH})_2$ molecules.²³ The bent M–O–H bond has been offered as a sign of covalent character,^{4,17} and in contrast, the more ionic group 2 metal dihydroxides have essentially linear M–O–H bonds.^{22,42} The experimental bond angles of CuOH (110.1°) and AgOH (107.8°) follow the same trend as that which we compute for $\text{Cu}(\text{OH})_2$ and $\text{Ag}(\text{OH})_2$, and AuOH has not yet been observed in the gas phase.

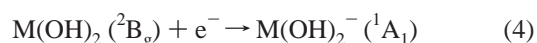
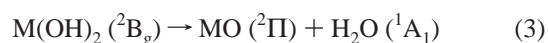
We conclude that solid $\text{Au}(\text{OH})_2$ will be a weak base. In contrast, the positive charge calculated on the barium center in the $\text{Ba}(\text{OH})_2$ molecule²² is approximately double that

computed for gold in the $\text{Au}(\text{OH})_2$ molecule, and the $\text{Ba}(\text{OH})_2$ molecule is ionic, and the solid is a strong base.^{22,42}

B3LYP calculations on the series of OMO dioxide molecules are only an approximation, but quartet states are lower in energy than doublet states.³⁴ However, the anti-symmetric O–M–O stretching frequencies for OCuO and OAuO in the doublet states are in accord with our observations, but the doublet OAgO state with the highest energy has an imaginary frequency and is not observed here. These calculations support the suggestion of stable high-energy quartet state intermediates for the excited metal atom reaction with O_2 and H_2 .

Reaction Mechanisms. The ground-state metal atoms appear to be unreactive toward insertion, as observed previously,^{3,7} but the excited metal atoms are reactive. Therefore, the insertion with hydrogen peroxide is straightforward for excited metal atoms, which are formed in the ablation process or by subsequent mercury arc irradiation.^{27,43} The $[\text{M}(\text{OH})_2]^*$ intermediate is relaxed by the matrix, and the dihydroxide molecule is stabilized. We observe a small yield of CuOH , AgOH , and AuOH upon sample deposition. The H_2O_2 reaction has been used as a source for CuOH molecules in a hollow cathode sputtering source with argon carrier gas,^{14,15} however, the dihydroxide molecule might be stabilized in a nozzle beam expansion experiment.

The same dihydroxide products are formed with the $\text{H}_2 + \text{O}_2$ reagent, and this reaction appears to proceed through the $[\text{OMO}]^*$ intermediate. We believe the $\text{M}(^2\text{P}) + \text{O}_2(^3\Sigma)$ reaction forms the $[\text{OMO}]^*$ intermediate in a quartet state for immediate reaction with adjacent H_2 molecules. Unreacted $[\text{OAgO}]^*$ decomposes upon relaxation to give AgO , but $[\text{OCuO}]^*$ and $[\text{OAuO}]^*$ relax to give the stable $^2\Pi_g$ states, which are observed here.^{7,28,34} The $\text{M}(\text{OH})_2$ molecules are very stable: reaction 2 is exothermic for ground-state metal atoms ($\Delta E = -111$, -66 , and -80 kcal/mol, respectively, for Cu , Ag , and Au). Furthermore, decomposition of the $\text{M}(\text{OH})_2$ molecules to the metal monoxide and water in gas-phase reaction 3 are endothermic processes ($\Delta E = 56$, 30, and 43 kcal/mol, respectively, for Cu , Ag , and Au). Note that $\text{Ag}(\text{OH})_2$ is the least stable and AgO is the only monoxide observed here (Figure 5). Finally, the $\text{M}(\text{OH})_2$ radicals have large electron affinities ($\text{EA} = 59$, 77, 73 kcal/mol, respectively) and form stable anions, reaction 4, and these anions can react favorably to make the $\text{M}(\text{OH})_4^-$ anions. Reaction 5 energies are exothermic (-45 , -29 , -40 kcal/mol, respectively). However, charged species are not major products in these systems.



(38) Reed, A. J.; Curtiss, L. A.; Weinhold, F. *Chem. Rev.* **1988**, *88*, 899.

(39) Frenking, G.; Fröhlich, N. *Chem. Rev.* **2000**, *100*, 717.

(40) Hotop, H.; Lineberger, W. C. *J. Phys. Chem. Ref. Data* **1985**, *14*, 73.

(41) Rosenbaum, N. H.; Owrutsky, J. C.; Tack, L. M.; Saykally, R. J. *J. Chem. Phys.* **1986**, *84*, 5308.

(42) Kaupp, M.; Schleyer, P. v. R. *J. Am. Chem. Soc.* **1992**, *114*, 491.

Conclusions

Reactions of laser-ablated Cu, Ag, and Au atoms with H_2O_2 and with $\text{O}_2 + \text{H}_2$ during condensation in excess argon give four new IR absorptions in each system (O–H stretch, M–O–H bend, O–M–O stretch, and M–O–H deformation) that are due to the $\text{M}(\text{OH})_2$ molecules, with weaker bands for the MOH molecules. Reagent isotopic substitution (D_2O_2 , $^{18}\text{O}_2$, $^{16}\text{O}^{18}\text{O}$, D_2 , and HD) and comparison with frequencies computed by the B3LYP density functional substantiate these vibrational assignments. The calculations converge to C_{2h} symmetry structures in the ${}^2\text{B}_g$ ground electronic state with $111\text{--}117^\circ$ M–O–H angles and reveal

(43) Gruen, D. M.; Bates, J. K. *Inorg. Chem.* **1977**, *16*, 2450.

substantial covalent character for these new metal dihydroxide molecules. The $\text{Au}(\text{OH})_2$ molecule is the most covalent in the series, owing to the effect of relativity and the high electron affinity of gold. We expect solid $\text{Au}(\text{OH})_2$ to be weak as a base. This matrix-isolation work provides the first experimental evidence for gold hydroxide molecules.

Acknowledgment. We appreciate support from NSF Grant CHE 03-52487 to L.A.

Supporting Information Available: Gold hydroxide anions, Figure S1 and Table S1. This material is available free of charge via the Internet at <http://pubs.acs.org>.

IC051201C